FOREX Publication
Open Access | Rapid and quality publishing

International Journal of
Electrical and Electronics Research (IJEER)
Research Article | Volume 10, Issue 2 | Pages 297-307 | e-ISSN: 2347-470X

Performance Analysis of Fault Tolerant Operation of PMSM using Direct Torque Control and Fuzzy Logic Control

Sandhya Kulkarni [1] and Archana Thosar [2]

[1]*Associate Professor, Department of Electrical Engineering, Govt. College of Engineering, Aurangabad, (M.S.), India, sskulkarni@geca.ac.in*
[2]*Professor, Department of Electrical Engineering, College of Engineering, Pune, India, archanagthosar@gmail.com*

***Correspondence:** Sandhya Kulkarni**:** sskulkarni@geca.ac.in

ABSTRACT- Electromagnets have traditionally been used in all drives. Because they take up space, the size of the machine grows in tandem with increased torque and it's rating thereby lowering its energy efficiency. If the rotor winding is replaced with permanent magnets, the motor will reverse. The recent improvement of magnetic materials resulted in a reduction in motor size and more effective use of redial space. Permanent Magnet Synchronous Motors (PMSM) have a high-power factor, are extremely durable, and require almost no maintenance. Such motors can be designed with power ranging from a few watts to a few kilowatts for applications ranging from fans to alternators including electric vehicles. This need reliable and safe operation of drives which would be fault tolerant. The study compares fault tolerant controllers using Direct Torque Control (DTC), and Fuzzy Logic Control (FLC) of PMSM for stator fault. Simulations are performed for different voltages and loads under fault. DTC selects voltage vectors using a hysteresis controller which gives better speed regulation but increases torque ripple requiring an accurate mathematical model. The use of FLC gives similar performance by precise voltage vector selection without needing an accurate mathematical model but has lower speed regulation. The results of DTC and FLC are show that even with failure of stator winding the motor can function satisfactorily.

Keywords: Direct torque control, fault control, Fuzzy logic Control, fault tolerance, PMSM.

ARTICLE INFORMATION
Author(s): Sandhya Kulkarni and Archana Thosar
Received: 27/04/2022; **Accepted**: 22/06/2022; **Published**: 28/06/2022;
e-ISSN: 2347-470X;
Paper Id: IJEER220427;
Citation: 10.37391/IJEER.100240
Webpage-link:
https://ijeer.forexjournal.co.in/archive/volume-10/ijeer-100240.html

Publisher's Note: FOREX Publication stays neutral with regard to Jurisdictional claims in Published maps and institutional affiliations.

1. INTRODUCTION

The ability to save energy is one of the most convincing arguments to adopt permanent magnet synchronous machines (PMSM). They have a high-power factor, efficient operation, tough design, and almost no maintenance. The use of magnets provides better use of radial space and eliminates the requirement for rotor winding, lowering rotor copper loss. Electrical drives can have a variety of faults. Appliances like air conditioning/heat pumps, electric automobiles, and industrial loads like pumping plants will accept such drive behavior. Electric drives may replace traditional mechanical actuators in automobiles to gain benefits such as increased efficiency and greater dynamic performance. Because of its adaptability, the PMSM is commonly used in industry which includes excellent efficiency and a high torque/weight ratio. The state-of-the-art of various electric drive faults is discussed in papers [1-3].

2. LITERATURE REVIEW

The development of FTC and the implementation of hardware methods necessitate the use of redundant sensors to deal with sensor failures. However, serious research in analytical solutions has been sought in the last two decades due to two major limitations of hardware design: high cost and increased space requirements. In comparison to DC motors and AC induction motors, PMSMs can provide the required precision while also meeting the need for high efficiency in a compact form. Sensors mounted on rotor shafts have several drawbacks, including lower reliability, noise susceptibility, increased cost and weight, and higher complexity that is entirely dependent on sensor accuracy.

Faults can occur at the machine's terminal or in winding. Machine current signature analysis (MCA) is a fault diagnostic method based on fast Fourier transform (FFT) analysis of stator current, but it is only applicable to steady-state operation [4-5]. It requires continuous stator current monitoring for at least one or more post-fault electrical periods. Park's vector approach is related to stator current analysis in a rotor reference frame and requires less computation time than MCA [6-7]. Some have proposed zero sequence current control through the use of a different combination of inverter bridges for fault detection at terminals [8]. Several authors [9–11] addressed model predictive control, finite element simulations for both normal and post fault operations with initial and next values using Parks' transform for multiphase PMSM with neutral, symmetrical component theory to detect fault. Fault tolerance is critical not only from a safety standpoint, but also from a reliability of drive.

FOREX Publication
Open Access | Rapid and quality publishing
International Journal of Electrical and Electronics Research (IJEER)
Research Article | Volume 10, Issue 2 | Pages 297-307 | e-ISSN: 2347-470X

Faults can occur at the machine's terminal or in winding. Machine current signature analysis (MCA) is a fault diagnostic method based on fast Fourier transform (FFT), analysis of stator current, but it is only applicable to steady-state operation [4-5]. It requires continuous stator current monitoring for at least one or more post-fault electrical periods. Park's vector approach is related to stator current analysis in a rotor reference frame and requires less computation time than MCA [6-7]. Some have proposed zero sequence current control through the use of a different combination of inverter bridges for fault detection at terminals [8]. Several authors [9-11] addressed model predictive control, finite element simulations for both normal and post fault operations with initial and next values using Parks' transform for multiphase PMSM with neutral, symmetrical component theory to detect fault. Fault tolerance is critical not only from a safety standpoint, but also from a reliability of drive.

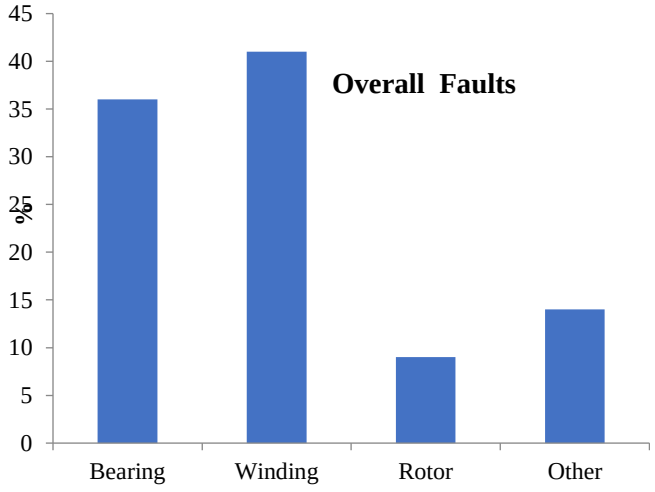

Figure 1: Faults in a Motor

Inverter faults are the focus of the majority of PMSM fault research. Several studies have been conducted on the use of inverters with an additional phase or neutral leg and a subsequent hardware configuration that increases complexity, size, and cost [12]. Furthermore, the neutral point of the machine must be accessible [13]. But among different faults, PMSM suffers mostly from stator faults and is less addressed. Objective of this work is application of 'fault tolerance' to a 3-ph PMSM for stator fault. Organization of paper is done in following way. *Section 2* contains information on classification of motor failures as well as the need for fault tolerance control along with literature review. The *Section 3* presents the methodology using a mathematical model of PMSM for a single-phase fault. In *Section 4*, how to use Park's transformation to design a controller using DTC is described for stator fault. The paper compares fault tolerant controllers using DTC and FLC for PMSM under stator fault. Results of simulation are presented cussed in *Section 5*. The discussion of results along conclusions, and its limitations are described in *Section 6*.

2.1 Classification of Faults

Faults occur as a result of overstressed and/or long-term operation of a drive. However, due to the extremely fast dynamics of PMSM motors, controlling them is a very difficult task. A fault tolerant machine is a machine- driven system that can continue to operate satisfactorily even after a fault occurs. Various faults that occur in PMSM are:

Electrical Faults

- Loss of phase in winding
- Phase-Ground Short circuit in winding
- Fault at the winding terminals
- Faults due to short circuit of turns

Faults in Inverter

- Open-circuit of power device
- Short-circuit of Power device

Mechanical Faults

- Broken in rotor bars faults
- Static and rotor eccentricity

Faults also occur in the rotor position sensor, direct current (DC) link power supply, and motor controller. Of the overall faults occurring in motor, faults in stator winding are the most common failures as shown from *Figure 1*. A single-phase fault is a common fault in windings, where the fault occurs on one of the phase windings.

In the 3-ph PMSM drive fed by voltage source inverter, faults in any of power switches may result in failure of the drive. But some critical applications require continuous operation (aerospace/electric vehicles *etc*). Hence such applications require an earlier fault detection, to isolate the failure and assure fault-tolerant control of the drive [14]. The threshold for a fault is determined empirically using detection methods. The threshold can be found within specific boundaries which simplifies parameterization [15]. Many papers discussed single-fault or three-phase fault separately. *Table 1*, gives comparative analysis of fault detection techniques. The paper discusses fault tolerant control for stator fault for the PMSM using DTC. This enables a motor control system to calculate the voltages that should be supplied to the stator in order to maximize torque under dynamic conditions.

Development of accurate mathematical model is sometimes difficult. For this (purpose) FLC is developed and results of both are compared. Due to paper space constraint mathematical analysis of 1-phase fault is discussed in paper.

FOREX Publication
Open Access | Rapid and quality publishing
International Journal of Electrical and Electronics Research (IJEER)
Research Article | Volume 10, Issue 2 | Pages 297-307 | e-ISSN: 2347-470X

Table 1: Comparative Analysis of Fault Detection Techniques

Types of faults in PMSM	Techniques used	Features	Demerits	Applications	Ref
Inverter faults	Designed using Triacs, IGBTs, MOSFETs, like inverter. Redundancy bidirectional fast fuse	Vector Control, Model Predictive Control, Observer based control	Use of control strategy, torque ripple is reduced	Short circuit, open-phase winding	[4],[5],[7], [10],[19]
Direct Torque Control	Relation between zero sequence, voltage and current by stator flux and stator voltage	High reliability; suitable for multiphase PMSMs	No need of vector co-ordinate transformation, Hysteresis controller	Stator faults, single phase, Open phase	[9],[15],[20]
Field Oriented	Space Vector based estimation of current	Control various faults for multi-phase machines, Low flux ripple, low torque	Increased cost; complex vector computation	Stator faults, single phase, Open phase, turn to turn short circuit	[1], [13], [14]

3. METHODOLOGY

Faults in armature or stator are usually related to insulation failure. There are two techniques to analyze faults, hardware methods and software methods. Hardware methods use different techniques like redundant leg, matrix converter, redundant switch, phase redundant topology, and cascade converter *etc.* to achieve fault tolerant control as shown in *Figure 2* and *Figure 3* for healthy and unhealthy three-phase system.

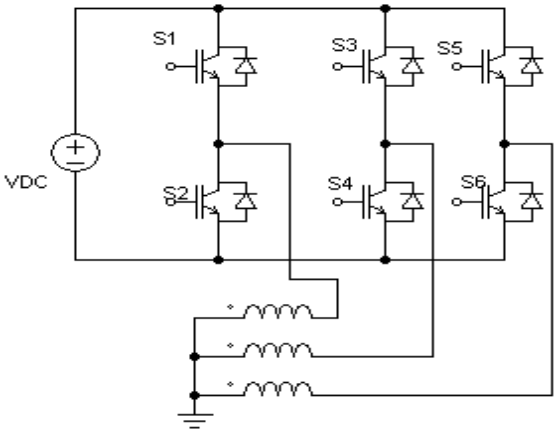

Figure 2: Inverter Fed 3-Phase PMSM without fault

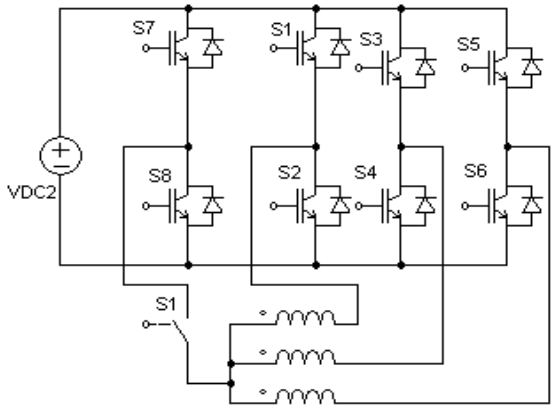

Figure 3: Inverter Fed 3 Phase PMSM with fault

Sensors and associated hardware must be mounted on the rotor for the hardware-based methods to work. Complex hardware makes systems bulky and increases operating costs, making them less beneficial [16]. As a result, fault tolerant control using a low-cost software configuration has recently become popular. This requires mathematical model, and use of voltage and current flux estimators, paper discusses fault tolerant operation of PMSM for single phase fault using Direct Torque Control.

3.1 Mathematical Model of PMSM under Healthy Condition

Phase failures can be caused by faults in motor windings. Let i_a, i_b, and i_c be the motor's 3-ph current, i_d, i_q, and i_0 be the motor current in the (d-q) frame and 'θ' be the rotor angle as expressed in *Equation 1*.

$$\begin{bmatrix} i_d \\ i_q \\ i_0 \end{bmatrix} = \frac{2}{3}\begin{bmatrix} \cos\theta & \cos\left(\theta-\frac{2\pi}{3}\right) & \cos\left(\theta+\frac{2\pi}{3}\right) \\ -\sin\theta & -\sin\left(\theta-\frac{2\pi}{3}\right) & -\sin\left(\theta+\frac{2\pi}{3}\right) \\ -\frac{1}{2} & -\frac{1}{2} & -\frac{1}{2} \end{bmatrix}\begin{bmatrix} i_a \\ i_b \\ i_c \end{bmatrix} \quad (1)$$

Equations (2) and (3) denote the neutral current and zero sequence current as:

$$i_0 = \frac{1}{3}(i_a + i_b + i_c) \quad (2)$$

$$i_n = i_a + i_b + i_c = 3i_0 \quad (3)$$

Under healthy conditions without fault, 3-ph current is symmetrical. So, i_n=0, therefore *Equation (3)* can be ignored.

3.2 Faulty Condition

Under the occurrence of single-phase fault on phase 'a' depicted in *Figure 4*, an immediate distortion occurs in zero sequence current. *Equations (4) and (5)* represents these equations of current as:

$$i_0 = i_q sin\theta - i_d cos\,\theta \quad (4)$$

$$i_n = 3i_0 = 3\,(i_q \sin\theta - i_d \cos\theta) \quad (5)$$

The magnitude neutral current is three-times the phase current under balanced condition and the phase angle difference is $\pi/6$ lead and lag for phases 'c' and 'b' respectively

FOREX Publication
Open Access | Rapid and quality publishing
International Journal of Electrical and Electronics Research (IJEER)
Research Article | Volume 10, Issue 2 | Pages 297-307 | e-ISSN: 2347-470X

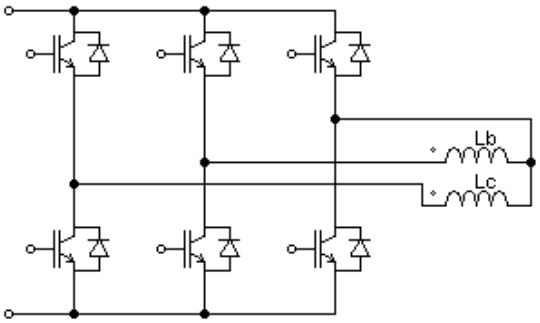

Figure 4: Single-phase fault on phase 'a'

3.3 Control Strategy

Electromagnetic torque remains constant during pre-fault and the post-fault period. Current for fault tolerant controller is derived using this principle for faulty phase, 'a'. By using *Equation (5),* transformed linear current and zero axis current are obtained in (*d-q*)-rotating frame of reference. It is computed from this voltage to compensate for torque ripple caused by phase fault. After a fault on phase '*a*,' the electromagnetic torque after and before occurrence of fault remain same. Hence, the magnitudes of '*b*' and '*c*'-phase currents are to be varied. Equation (6) represents the expression for electromagnetic torque of PMSM in the *dq*- system.

$$T_e = \frac{3}{2} p[\Psi_m \, i_q + (L_d - L_q) i_d i_q] \quad (6)$$

Where 'p' be the number of pole pairs. By assuming same values of inductance of direct and quadrature axis inductance, $L_d = L_q$, and i_d, i_q be stator currents in (*d-q*)-rotating frame of reference. *Equation (7),* denotes the simplified equation of electromagnetic torque.

$$T_e = \frac{3}{2} p \Psi_m \, i_q \quad (7)$$

As seen from *Equation (7),* the electromagnetic torque of motor is mainly controlled by i_q, quadrature axis current. When a single-phase to ground fault occurs (here on phase '*a*') i_0, zero sequence current will not be zero. But its magnitudes are $i_0 = -I_m \sin(\theta)$; $i_d = 0$; and $i_q = -I_m$. The zero- sequence current must be altered at this time. As the change is in i_0, zero sequence current; the magnitudes of direct and quadrature axis currents, i_d, i_q remain unchanged. Thus, change of i_0, zero sequence current keeps the (*d-q)* axis currents unchanged. Its corresponding magnitudes of the zero-sequence voltage after single-phase fault is given by *Equations (8) and (9).*

$$V_0 = R_s i_0 + L_0 \frac{di_0}{dt} \quad (8)$$

Equation (5) shows that the post fault zero-sequence current is alternating and sinusoidal in nature. Let, V_d, V_q be stator voltages in (*d-q*) rotating frame of reference. R_s denotes stator resistance. Ψ_d and Ψ_q represents flux linkages, L_d, L_q be the direct and quadrature inductances in (*d-q)*-rotating frame of reference. Magnet flux linkage is represented by Ψ_m. Under balanced steady-state operation of motor, the motor rotates at a constant torque and speed, then *dq* quantities will become DC quantities. Thus, the time varying components will be zero. *Equation (9)* and (10) gives stator voltage in terms of V_d, V_q, transformed control voltage in *dq*-frame of reference.

$$V_d = R_s i_d - L_q i_q \omega_e + L_d \frac{di_d}{dt} \quad (9)$$

$$V_q = R_s i_q + L_d i_d \omega_e + \omega_e \Psi_m + L_q \frac{di_q}{dt} \quad (10)$$

Equation (11) shows that voltage, zero sequence voltage, V_0 under single-phase fault is a controlled by direct axis current, quadrature axis current, speed, and rotor angle θ. Hence, V_0 is function of i_d and i_q.

$$V_0 = (R_s i_q + L_0 i_d \omega_e) sin\theta + (-R_s i_d + L_0 i_q \omega_e) cos\theta \quad (11)$$

4. FAULT TOLERANT PMSM FOR SINGLE PHASE FAULT USING DTC

Recently, DTC has been considered as a viable alternative to vector control of alternating current drives. DTC eliminates the requirement to transform complex vector coordinates. The stator flux linkages are accurately monitored and used as a directional flux coordinate. The instantaneous slip between the stator and rotor fluxes determines the rate of change of torque in classical DTC. It is well-known for its torque and flux control, which is both quick and dependable. Correct stator voltage vectors can be used to increase or decrease stator flux [17]. As a result, direct modification of stator voltage is carried out in response to flux and torque errors to achieve simultaneous control of flux and torque. DTC improves dynamic performance by avoiding indirect torque control through the flux component of current in vector control by selecting correct voltage vectors based on stator flux linkage, torque, and stator flux angle [18]. Park's vector approach is based on a rotor frame of reference analysis of stator current. DTC includes the flux estimator, torque estimator, hysteresis controller, switching table, and proportional integral (PI) controller. To estimate flux and current enable flux, a mathematical model for a single-phase fault is developed [19].

4.1 Stator voltage equations in abc system

Let the stator three-phase self-inductances and mutual inductances be of same value as $L_a = L_b = L_c = L$ and $M = M_{ca} = M_{bc} = M_{ab} = M$ mutual inductance. When fault occurs on phase '*a*', stator flux-linkages are given by *Equations (12) to (14)* on stator side and *Equations (15) to (17)* on rotor side.

$$\Psi_{sa} = Li_a + Mi_b \quad (12)$$

$$\Psi_{sb} = Li_b + Mi_c \quad (13)$$

$$\Psi_{sc} = Li_c + Mi_a \quad (14)$$

Figure 5 depicts flux linkages of 3- in *abc*-frame given by.

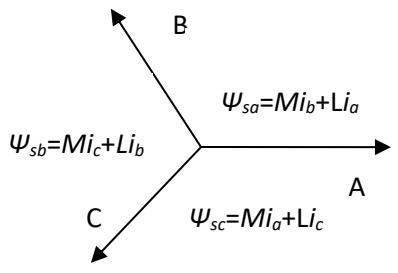

Figure 5: Flux linkages of three phases in abc form

FOREX Publication
Open Access | Rapid and quality publishing
International Journal of Electrical and Electronics Research (IJEER)
Research Article | Volume 10, Issue 2 | Pages 297-307 | e-ISSN: 2347-470X

$$\Psi_a = \Psi_{sa} + \Psi_m \cos\theta_r \quad (15)$$
$$\Psi_b = \Psi_{sb} + \Psi_m \cos(\theta_r - 120^0) \quad (16)$$
$$\Psi_c = \Psi_{sc} + \Psi_m \cos(\theta_r + 120^0) \quad (17)$$

Let '*a*', '*b*', and '*c*' are the components of stator flux-linkages caused by stator currents and the rotor along the *a, b,* and *c* axes, respectively. θ_r and λ_m are the electrical angular rotor positions with respect to phase '*a*' and permanent magnet flux. *Equations (18) to (20)* represents the stator voltage equations V_a, V_b, and V_c.

$$V_a = 0i_b + 0i_c + \frac{d\Psi_a}{dt} \quad (18)$$
$$V_b = R_b i_b + 0i_c + \frac{d\Psi_b}{dt} \quad (19)$$
$$V_c = 0i_b + R_c i_c + \frac{d\Psi_c}{dt} \quad (20)$$

Where V_a, V_b and V_c be stator voltages and R_a R_b, R_c are stator resistances. Assuming fault is occurring on phase, '*a*', hence by neglecting voltage V_a, resulting voltage is given by *Equation 21*.

$$\begin{bmatrix} V_b \\ V_c \end{bmatrix} = \begin{bmatrix} R_b & 0 \\ 0 & R_c \end{bmatrix}\begin{bmatrix} i_b \\ i_c \end{bmatrix} + \begin{bmatrix} L & M \\ M & L \end{bmatrix}\begin{bmatrix} \frac{di_b}{dt} \\ \frac{di_c}{dt} \end{bmatrix} - \begin{bmatrix} \Psi_m \omega_r \sin\left(\theta_r - \frac{2\pi}{3}\right) \\ \Psi_m \omega_r \sin\left(\theta_r - \frac{2\pi}{3}\right) \end{bmatrix} \quad (21)$$

4.2 Flux and Current Estimators

In DTC, flux estimator and current estimator are used. The former includes an integrator that is sensitive not only to DC offset voltage but also to the initial value [20-21]. Higher DC offset combined with improper initial values might cause saturation problem. This may lead to whole system becoming unstable system. The current and flux estimators, on the other hand, are able to overcome this issue. Monitoring of phase currents can be used to calculate the associated currents. As a result, the focus of this paper is on the latter. There are two different types of current model flux estimators: one in 2-phase stationary (α-β) system and another in 2-phase rotating (*d*-*q*) system. Therefore, the current and flux estimator applied in a fault-free PMSM cannot be applied straight to a faulty one. It needs modification. The following are the modified flux estimators that are effective for fault tolerant DTC [21-22].

4.3 Modified Current Model Flux Estimator

The flux linkages Ψ_α, Ψ_β are given by the stator current in stationary $\alpha\beta$-system expressed in *Equation 22.*

$$\begin{bmatrix} \Psi_{s\alpha} \\ \Psi_{s\beta} \end{bmatrix} = \begin{bmatrix} \frac{1}{2}(M-L) & \frac{1}{2}(M-L) \\ \frac{\sqrt{3}}{2}(L-M) & -\frac{\sqrt{3}}{2}(L-M) \end{bmatrix}\begin{bmatrix} i_b \\ i_c \end{bmatrix} \quad (22)$$

In ($\alpha\beta$)- stationary system, stator current, i_α and i_β given by *Equation 23.*

$$\begin{bmatrix} i_\alpha \\ i_\beta \end{bmatrix} = \begin{bmatrix} -\frac{1}{3} & -\frac{1}{3} \\ \frac{\sqrt{3}}{3} & -\frac{\sqrt{3}}{3} \end{bmatrix}\begin{bmatrix} i_b \\ i_c \end{bmatrix} \quad (23)$$

Hence, *equation (22)* is re-written by *Equation 24.*

$$\begin{bmatrix} \Psi_\alpha \\ \Psi_\beta \end{bmatrix} = \begin{bmatrix} \Psi_{s\alpha} \\ \Psi_{s\beta} \end{bmatrix} + \frac{2}{3}\begin{bmatrix} \Psi_m cos\,\theta_r \\ \Psi_m sin\,\theta_r \end{bmatrix} \quad (24)$$

where $\Psi_s = \sqrt{\Psi_\alpha^2 + \Psi_\beta^2}$

Electromagnetic torque in two-phase, stationary system is given by *Equation 25.*

$$T = \frac{3}{2}p\,(\Psi_\alpha\, i_\beta - \Psi_\beta i_\alpha) \quad (25)$$

Here, *p* be number of pole pairs.

Equation (24) gives flux-linkages, Ψ_d and Ψ_q.

$$\begin{bmatrix} \Psi_d \\ \Psi_q \end{bmatrix} = \begin{bmatrix} L_d & 0 \\ 0 & L_q \end{bmatrix}\begin{bmatrix} i_d \\ i_q \end{bmatrix} + \begin{bmatrix} \Psi_m \\ 0 \end{bmatrix} \quad (26)$$

Equation gives i_d and i_q using Clarke and Park's transformations (25).

$$\begin{bmatrix} i_d \\ i_q \end{bmatrix} = \begin{bmatrix} \cos\theta_r & -\sin\theta_r \\ sin\theta_r & \cos\theta_r \end{bmatrix}\begin{bmatrix} -1/2 & -1/2 \\ \sqrt{3}/2 & -\sqrt{3}/2 \end{bmatrix}\begin{bmatrix} i_b \\ i_c \end{bmatrix} \quad (27)$$

The magnitude of stator flux linkage Ψ_s is expressed as, $\Psi_s = \sqrt{{\Psi_d}^2 + {\Psi_q}^2}$

The electromagnetic torque exerted in a (*d*-*q*)-rotating system is given by *Equation 28.*

$$T_e = \frac{3p[\Psi_m i_q + (L_d - L_q) i_d i_q}{2} \quad (28)$$

As value of mutual inductance, M = half of self-inductance L, as shown in *Equation 29.*

$$L_d = L_q = L + \frac{1}{2}L = \frac{3}{2}L \quad (29)$$

4.3 DTC Controller

The primary goal of fault tolerant DTC for PMSM after a single-phase fault is to control motor current and torque to maintain set limits. *Figure 6* shows a simplified block design of a fault tolerant PMSM for a single-phase fault using DTC. It has flux and torque estimators, hysteresis, and a PI controller, as well as an inverter in the power unit. PI controller regulates rotor speed and assists in accelerating rotor speed to time to reach by mitigating steady-state error. This same torque and stator flux linkage are adjusted by the hysteresis controller through the proper selection of voltage vectors. If the torque or flux deviation from the reference exceeds the allowable tolerance, the inverter's IGBTs are tripped [23].

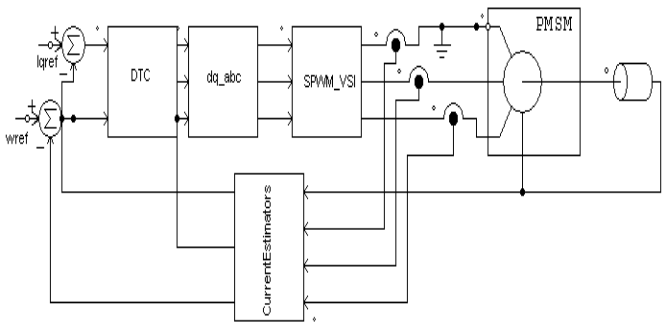

Figure 6: Block diagram DTC based Fault Tolerant Controller

4.4 Fuzzy Logic Controller Fed PMSM

DTC uses a hysteresis controller to regulate flux, which has torque ripples that increase in dynamic conditions such as a phase fault. FLC replaces the hysteresis controller in this case. The inputs are stator flux angle, stator flux linkage errors, and electromagnetic torque, while the outputs are voltage vectors.

FOREX Publication
Open Access | Rapid and quality publishing
International Journal of Electrical and Electronics Research (IJEER)
Research Article | Volume 10, Issue 2 | Pages 297-307 | e-ISSN: 2347-470X

In every plane sextant region, each voltage vector is symmetrical. As a result, by examining the state in a single sextant region, all of the rules can be deduced. *Equation (30),* was used to map the entire plane of 360^0 for reducing the number of fuzzy reasoning rules. It is divided into three sections: fuzzification, fuzzy reasoning, and defuzzification.

$theta = \theta - \frac{\pi}{3}(\frac{\theta+\frac{\pi}{6}}{\frac{\pi}{3}})$ (30), where *theta* represents the actual input of the fuzzy controller and 'θ' be its real stator flux angle [24-25].

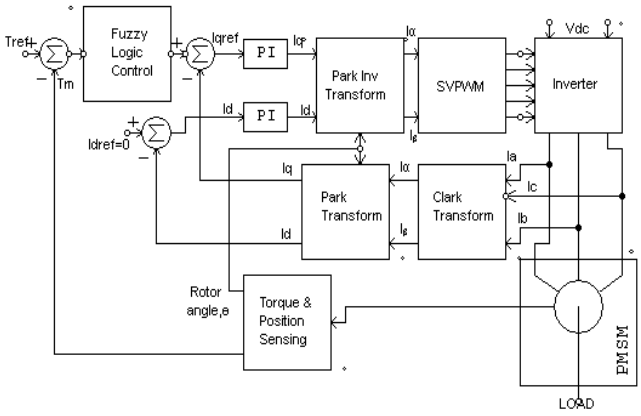

Figure 7: Block diagram of FLC

Table 2: Parameters of PMSM

Parameters	Values
R_s, Stator Resistance per phase	4.3Ω
L_d, Inductance direct axis	7.5mH
L_q, Inductance quadrature axis	7.5mH
Number of poles	4
Voltage/ph	300V
T, Rated torque	2Nm
J, Moment of Inertia	0.00179Kgm^2

5. RESULTS

PMSM with a pump as load is taken as an example to simulate the result for faulty condition for PMSM whose parameters are given in above *Table 2.* Simulations are carried out using MATLAB-Simulink platform. Reference speed of motor is set to 1500rpm. Results of simulations for single-phase to ground fault are tabulated in *Table 3*. Few simulations result for phase-ground fault are shown in *Figures 8-10.* Fault is applied at T=1.6 sec for 0.04 second interval of time. *Figure 8* shows variation of speed and electromagnetic torque under single-phase fault. It causes the change of torque, percentage of torque ripple; change of speed, as a percentage of speed ripple. This results in change of stator current, i_{abc} as shown in *Figure 9.* Then system restores at T=1.64 second as shown in *Figure 9.* Simulations are performed for variable voltage and variable load condition. Simulation with 20% higher rated voltage for 3-phase fault for speed and electromagnetic torque is shown in *Figure10a*, whose magnified waveform of change in speed, change in torque waveform is shown in *Figure10b* whereas *Figure 11* shows stator current when fault is applied at T=1.6sec for duration of 0.04sec. These simulation results are tabulated in *Table 3.*

(i) **T_L=8Nm, V=300, 1ph - Fault -DTC**

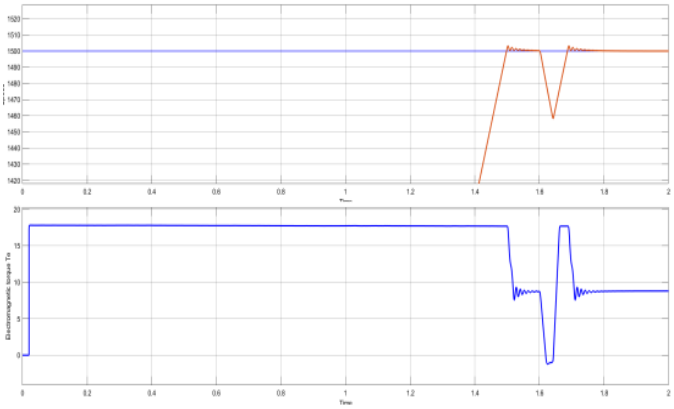

Figure 8: Speed and Torque

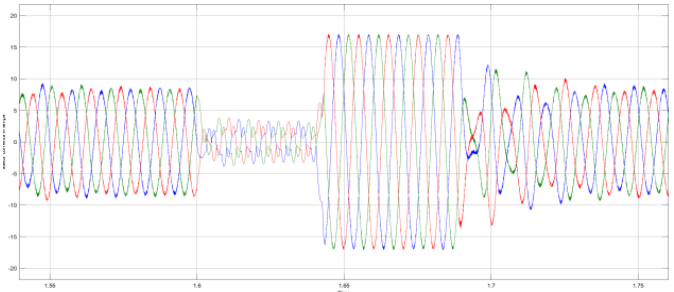

Figure 9: Stator current

(ii) **V_{dc}=350V, T_L-6Nm,1- phase fault-DTC**

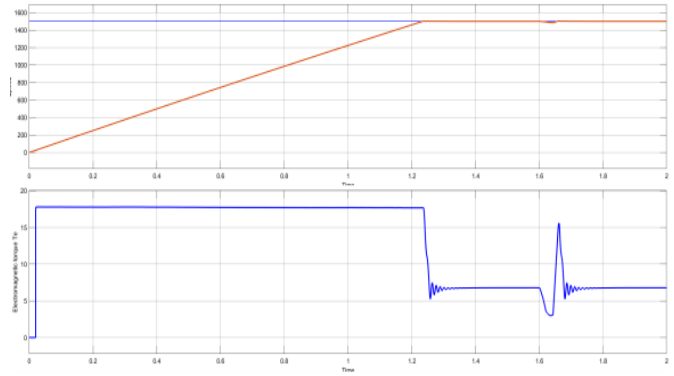

Figure 10 (a): Speed and Torque

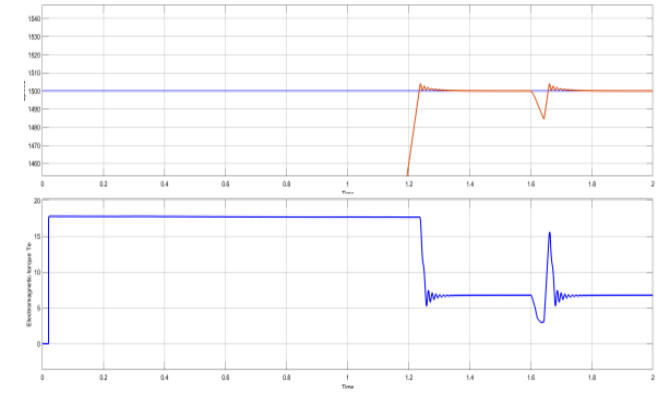

Figure 10 (b): Magnified Speed and Torque

FOREX Publication
Open Access | Rapid and quality publishing
International Journal of Electrical and Electronics Research (IJEER)
Research Article | Volume 10, Issue 2 | Pages 297-307 | e-ISSN: 2347-470X

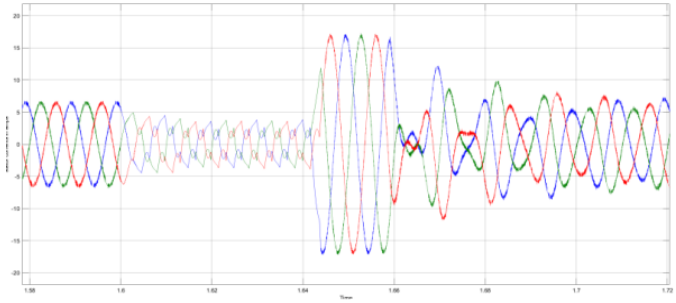

Figure 11: Stator current

Fuzzy rules are designed for PMSM to operate on normal and under different fault conditions. After obtaining the FLC output voltage vector, it is transformed to drive the inverter fed PMSM. Due to paper constraints, these methods are not discussed in depth. To make comparison clearer, for FLC also the fault is applied at T=1.6 sec for an interval of 0.04 sec. *Figure 12* shows waveforms for variation in stator current, i_{abc}; *Figure 13* shows variation of electromagnetic torque and speed, indicating fault free, faulty and fault cleared operation of motor. *Figure 14* compares the time to reach steady-state for DTC and FLC; as observed from *Figure*, FLC reaches steady state quickly than DTC but with a reduced speed than set speed, whereas DTC gives better speed regulation but takes longer time to reach steady state. With reduction in DC link voltage there is considerable reduction in stator current ripple and torque ripple. Its analysis is shown in *Table 3*.

(i) **T_L=8 Nm, V=300, Stator 1ph Fault - FLC controller**

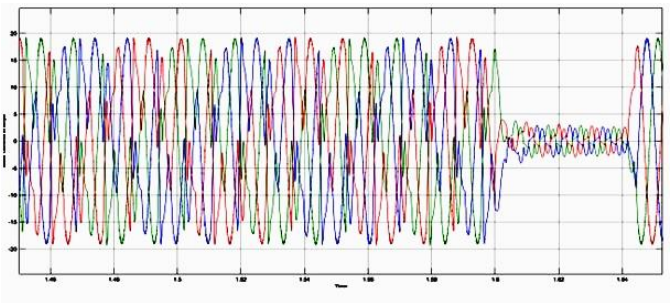

Figure 12: Stator Current

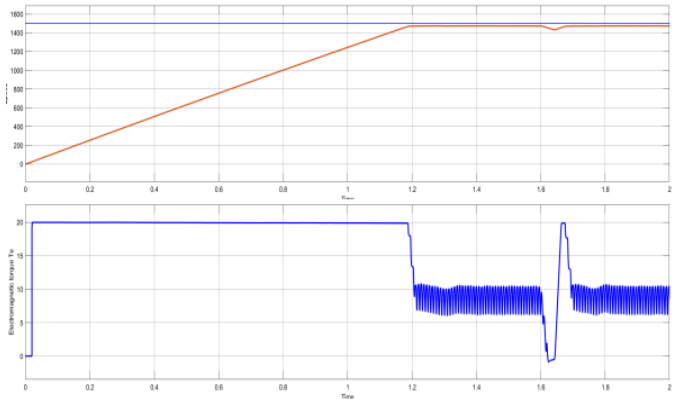

Figure 13: Speed and Torque

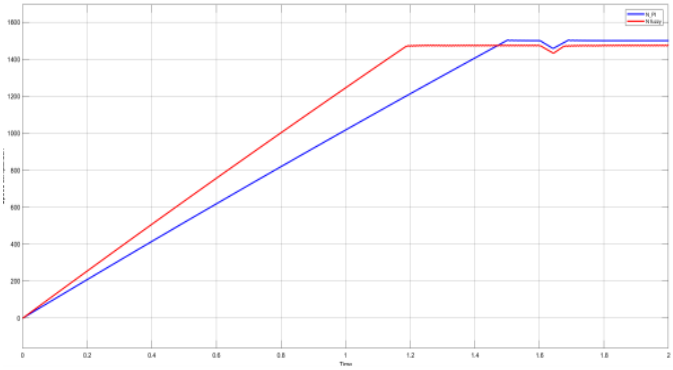

Figure 14: Comparison between DTC and Fuzzy steady state reach time

Figure 15 a, b shows simulation waveforms for speed and torque at 20% higher voltage, speed ripple is high when phase fault applied at T=1.6sec for an interval of 0.04 second. The change in stator current is shown in *Figure 16* and comparison of DTC and FLC to reach steady state time is shown in *Figure 17*.

(i) **V_{dc}=350V, T_L-6Nm**

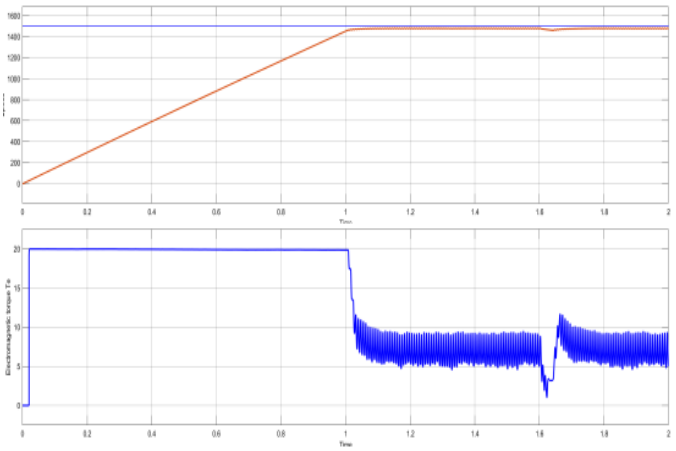

Figure 15 (a): Speed and Torque

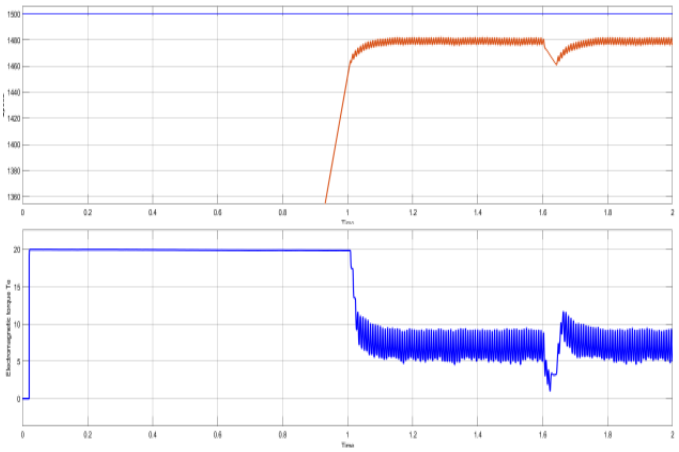

Figure 15b: Magnified Speed and Torque

FOREX Publication
Open Access | Rapid and quality publishing
International Journal of Electrical and Electronics Research (IJEER)
Research Article | Volume 10, Issue 2 | Pages 297-307 | e-ISSN: 2347-470X

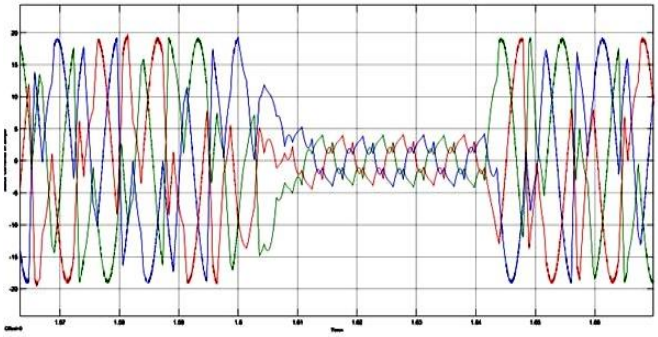

Figure 16: Stator current

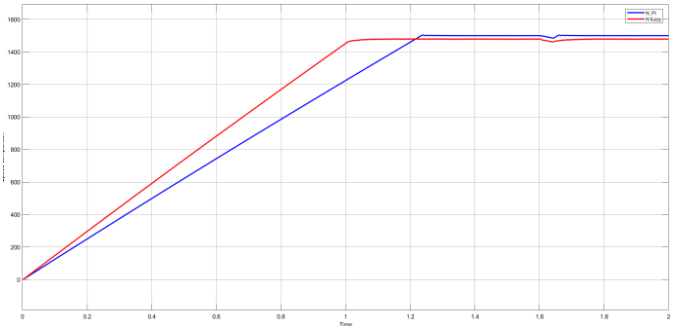

Figure 17: Time to reach steady state

Table 3: Simulation Results for Phase -Ground Fault

Controller	Voltage Variation	Stator current in A		Current ripple	Torque in Nm		Torque Ripple	Speed in rpm		Change in Speed	Time to set	Rotor angle
	V	Imax	Imin	%	Tmax	Tmin	%	Nmax	Nmin	%	Sec	Rad
DTC	220(15% derated)	4.5	2.5	44.4	5	3	40	1500	1485	1	0.9	240
	250(10% derated)	9	5	44.4	10	6	40	1500	1480	1.4	1.16	235
	300-rated	14	7.5	46.4	12	7	41.7	1500	1485	1	1.22	230
	350 -(120%)	15	8	46.7	14	8	42.9	1500	1480	1.4	1.46	235
Fuzzy	220(15% derated)	7	4	42.9	4.5	3	33.3	1500	1480	1.3	0.78	240
	250(10% derated)	11	6	45.5	7.5	5	33.3	1500	1475	1.7	0.84	240
	300-rated	14	7.5	46.4	12	7	41.7	1500	1478	1.5	0.88	240
	350 -(120%)	16	9	43.8	13	8	38.5	1500	1478	1.5	1	240

Simulation analysis of *Table 2* is shown in *Figures18-21*

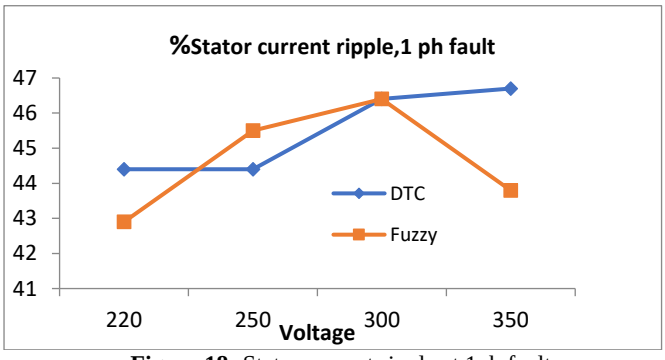

Figure 18: Stator current ripple at 1ph fault

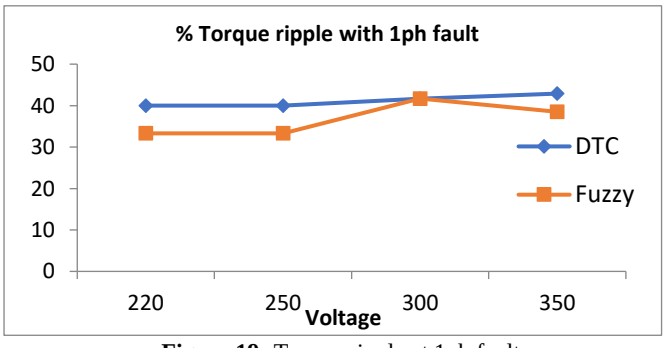

Figure 19: Torque ripple at 1ph fault

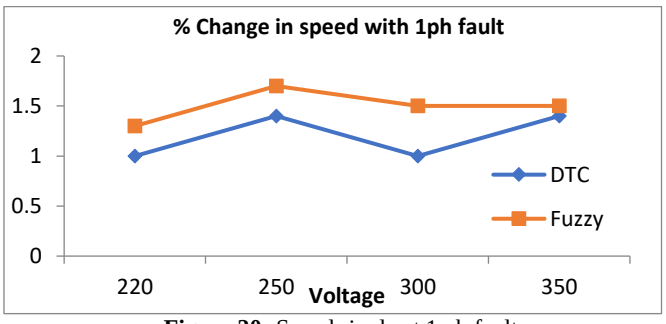

Figure 20: Speed ripple at 1 ph fault

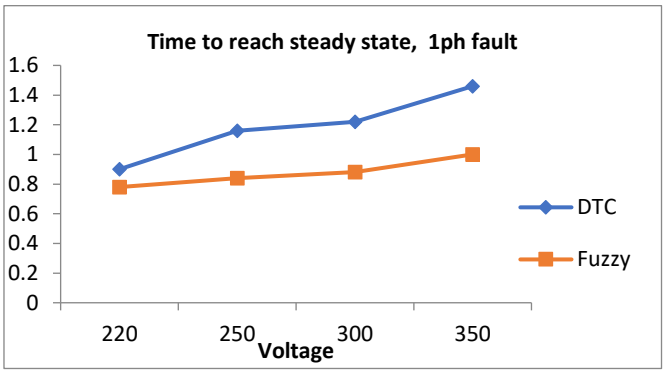

Figure 21: Time to reach steady state at 1ph fault

FOREX Publication
Open Access | Rapid and quality publishing
International Journal of Electrical and Electronics Research (IJEER)
Research Article | Volume 10, Issue 2 | Pages 297-307 | e-ISSN: 2347-470X

Simulation results for single phase to ground fault shows that stator current ripple and torque ripple content are more or less same but FLC reaches steady state quickly compared to DTC as shown from *Figure 21*. In DTC, ripple content of speed is less compared to FLC as seen from *Figure 20.*

Table 4: Simulation Results for Three Phase Ground fault (with voltage variation)

Controller	Voltage variation	Stator Current in A		Current ripple	Torque Nm		Torque Ripple	Speed in rpm		Change in Speed	Time to set	Rotor angle
	V	Imax	Imin	%	Tmax	Tmin	%	Nmax	Nmin	%	sec	rad
DTC	200	14	6	57.1	17	6	64.7	1500	1440	4	1.16	235
	220	14	6.5	53.6	15	5	66.7	1500	1450	3.4	1.16	235
	250	15	7	53.3	17	6	64.7	1500	1445	3.7	1.14	235
	300	15	7.5	50	17	7	58.8	1500	1460	2.7	1.14	235
	350	17	8	52.9	18	7	61.1	1500	1460	2.7	1.14	235
Fuzzy	200	14	6.5	53.6	12	5	58.3	1480	1430	3.4	0.9	240
	220	15	7	53.3	15	6	60	1475	1420	3.7	0.88	240
	250	14	7.5	46.4	17	8	52.9	1470	1420	3.4	0.86	240
	300	16	7.5	53.1	17	7	58.8	1470	1440	2	0.86	240
	350	18	8	55.3	17	7	58.8	1470	1438	2.2	0.86	240

Simulation analysis of *Table 4* is in shown in *Figures 22-25.*

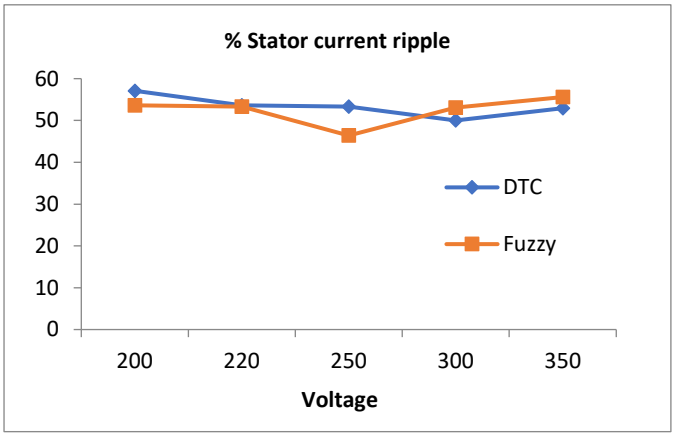

Figure 22: Stator current ripple at 3ph fault

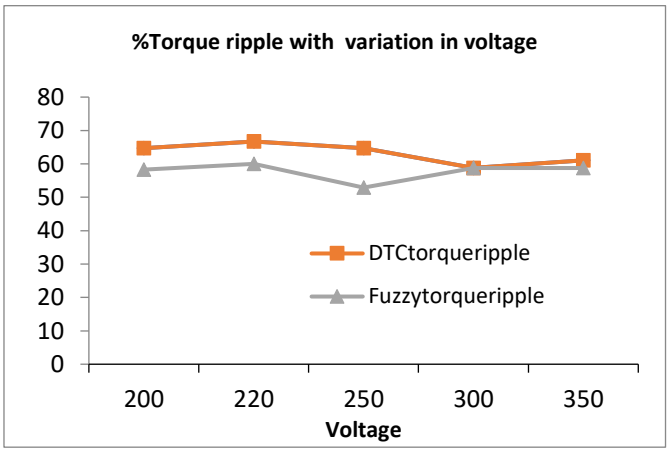

Figure 24: Torque ripple at 3ph fault

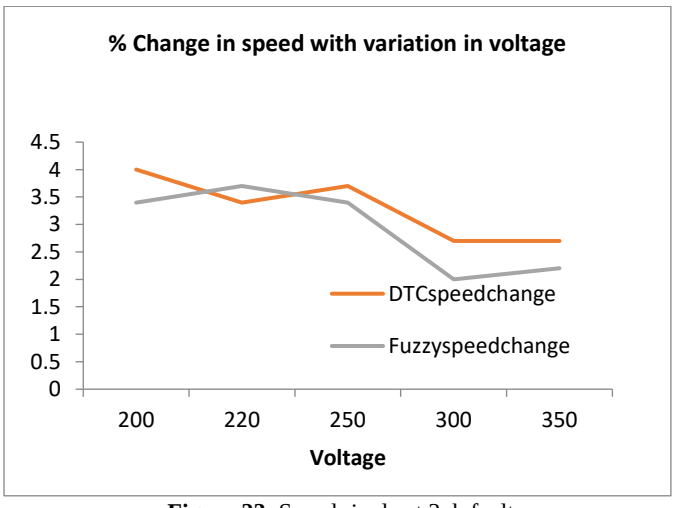

Figure 23: Speed ripple at 3ph fault

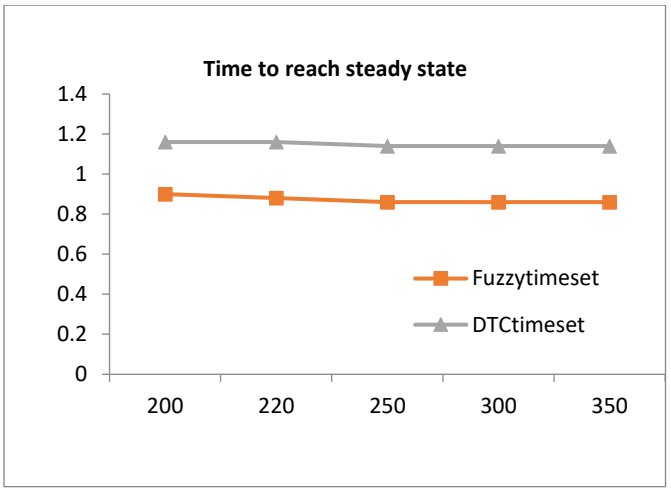

Figure 25: Time to reach steady state at 3ph fault

FOREX Publication
Open Access | Rapid and quality publishing
International Journal of Electrical and Electronics Research (IJEER)
Research Article | Volume 10, Issue 2 | Pages 297-307 | e-ISSN: 2347-470X

5. CONCLUSION

The paper discusses fault-tolerant control using DTC and FLC for single-phase fault and three-phase fault for PMSM. It is based on a mathematical model for the healthy and faulty condition of a three-phase PMSM. Fault tolerant controller is designed using DTC and FLC, whose results are tabulated in *Table 2 and 3*. Results of *Table 2* show that, DTC gives maximum torque ripple of 40% and current ripple of 44% for single-phase to ground fault whereas these values rise to 57.1% and 66% for three-phase to ground fault. FLC reaches to steady state earlier than DTC as seen from *Figures 14 and 17*, and has lower stator current ripple compared to DTC. Percentage change in speed for both controllers is almost same. Fault causes stator current ripple, high torque ripples and current unbalance in system and motor windings may lead to drawing high circulating current. Analysis of simulation results shows that DTC has higher torque ripple but better speed regulation, as tuning is done by PI controller and does not require co-ordinate transform.

Hence, designing control become quite simpler. Whereas FLC gives faster response, reach steady-state quite early than DTC but has poor speed regulation. Still results of both are comparable.

Under dynamic conditions, as PMSMs have different configuration, slot/pole combinations, and become non-linear. This adversely affects development of accurate model which will affect performance of DTC. All of these factors have an impact on the correctness of the technique and an accurate fault estimation, and determination.

The proposed method has the advantage of being able to detect and identify faults in a few sample intervals, as well as identifying other faults using the same model motor performance. The effect of fault tolerant DTC in a *dq*-rotating system using a current and flux estimator is identical to field-oriented control, but it lowers model complexity. FLC is rule based, will be considered as an obvious choice when developing mathematical model would be too difficult as results of both are similar. Control parameters like electromagnetic torque ripple, stator current ripple is analysed. Method suffers from accurate determination of fault threshold accurately, uncertainty at higher voltage. It can be fully utilized especially in electric vehicles, when continuing operation is necessary after a defect until a safe stop and current control is achieved. As a result, the proposed strategy is effective.

ACKNOWLEDGEMENTS

Authors would like to thank Government College of Engineering, Aurangabad, (M.S.), India, for support and research facility.

REFERENCES

[1] Tousizadeh M, Che HS, Selvaraj J, Abd Rahim N, Ooi BT. Fault-tolerant field-oriented control of three-phase induction motor based on unified feedforward method. IEEE Transactions on Power Electronics. 2018 Dec 3;34(8):7172-83.

[2] Gan C, Chen Y, Qu R, Yu Z, Kong W, Hu Y. An overview of fault-diagnosis and fault-tolerance techniques for switched reluctance machine systems. IEEE Access. 2019 Nov 28;7: 174822-38.

[3] Tian B, Mirzaeva G, An QT, Sun L, Semenov D. Fault-tolerant control of a five-phase permanent magnet synchronous motor for industry applications. IEEE Transactions on Industry Applications. 2018 Mar 27;54(4):3943-52.

[4] Amin AA, Hasan KM. A review of fault tolerant control systems: advancements and applications. Measurement. 2019 Sep 1; 143:58-68.

[5] Yang H, Han QL, Ge X, Ding L, Xu Y, Jiang B, Zhou D. Fault-tolerant cooperative control of multiagent systems: A survey of trends and methodologies. IEEE Transactions on Industrial Informatics. 2019 Oct 1;16(1):4-17.

[6] Bourogaoui M, Sethom HB, Belkhodja IS. Speed/position sensor fault tolerant control in adjustable speed drives–A review. ISA transactions. 2016 Sep 1; 64:269-84.

[7] I. Jlassi, J. O. Estima, S. K. El Khil, N. M. Bellaaj, and A. J. M. Cardoso, "A robust observer-based method for IGBTs and current sensor fault diagnosis in voltage-source inverters of PMSM drives," IEEE Transactions on Industry Applications, vol. 53, no. 3, pp. 2894–2905, 2016.

[8] Kommuri S. K., Defoort M, Karimi HR, Veluvolu KC. A robust observer-based sensor fault-tolerant control for PMSM in electric vehicles. IEEE Transactions on Industrial Electronics. 2016 Jul 13;63(12):7671-81.

[9] Kao IH, Wang WJ, Lai YH, Perng JW. Analysis of permanent magnet synchronous motor fault diagnosis based on learning. IEEE Transactions on Instrumentation and Measurement. 2018 Jun 29;68(2):310-24.

[10] Arafat AK, Choi S, Baek J. Open-phase fault detection of a five-phase permanent magnet assisted synchronous reluctance motor based on symmetrical components theory. IEEE Transactions on Industrial Electronics. 2017 Mar 14;64(8):6465-74.

[11] Hang J, Ding S, Zhang J, Cheng M, Wang Q. Open-phase fault detection in delta-connected PMSM drive systems. IEEE Transactions on Power Electronics. 2017 Nov 13;33(8):6456-60.

[12] Wang S, Bao J, Li S, Yan H, Tang T, Tang D. Research on interturn short circuit fault identification method of PMSM based on deep learning. 22nd International Conference on Electrical Machines and Systems (ICEMS) 2019 Aug 11 (pp. 1-4). IEEE.

[13] Wentao Huang, Wei Hua, Fuyang Chen, Mingjin Hu, and Jianguo Zhu. Model Predictive Torque Control with SVM for Five-Phase PMSM under Open-Circuit Fault Condition. IEEE Transactions on Power Electronics. 2020 May, 35(5):5531–5540.

[14] Quiroz JC, Mariun N, Mehrjou MR, Izadi M, Misron N, Radzi MA. Fault detection of broken rotor bar in LS-PMSM using random forests. Measurement. 2018 Feb 1;116: 273-80.

[15] M Rupesh, Dr. T S Vishwanath (2021), Fuzzy and ANFIS Controllers to Improve the Power Quality of Grid Connected PV System with Cascaded Multilevel Inverter. IJEER 9(4), 89-96. DOI: 10.37391/IJEER.090401.

[16] Liang S, Chen Y, Liang H, Li X. Sparse representation and SVM diagnosis method for inter-turn short-circuit fault in PMSM. Applied Sciences. 2019 Jan;9(2):224.

[17] Armin M, Roy PN, Das SK. A survey on modelling and compensation for hysteresis in high-speed nano-positioning of AFMs: Observation and future recommendation. International Journal of Automation and Computing. 2020 Apr 14:1-23.

[18] Wang X, Wang Z, Xu Z, Cheng M, Wang W, Hu Y. Comprehensive diagnosis and tolerance strategies for electrical faults and sensor faults in dual three-phase PMSM drives. IEEE Transactions on Power Electronics. 2018 Oct 16;34(7):6669-84.

[19] Zhang J, Zhan W, Ehsan M. Fault-tolerant control of PMSM with inter-turn short-circuit fault. IEEE Transactions on Energy Conversion. 2019 Aug 20;34(4):2267-75.

[20] Zhou X, Sun J, Li H, Lu M, Zeng F. PMSM open-phase fault-tolerant control strategy based on four-leg inverter. IEEE Transactions on Power Electronics. 2019 Jul 1;35(3):2799-808.

International Journal of
Electrical and Electronics Research (IJEER)
Research Article | Volume 10, Issue 2 | Pages 297-307 | e-ISSN: 2347-470X

[21] Chai F, Gao L, Yu Y, Liu Y. Fault-tolerant control of modular permanent magnet synchronous motor under open-circuit faults. IEEE Access. 2019 Oct 21;7: 154008-17.

[22] Bouchareb C, Nait-Said MS. PMSM model with phase-to-phase short-circuit and diagnosis by ESA and EPVA. Advances in Electrical and Electronic Engineering. 2016 Dec 31;14(5):522-30.

[23] Yan H, Xu Y, Cai F, Zhang H, Zhao W, Gerada C. PWM-VSI fault diagnosis for a PMSM drive based on the fuzzy logic approach. IEEE Transactions on Power Electronics. 2018 Mar 9;34(1):759-68.

[24] He S, Shen X, Jiang Z. Detection and location of stator winding interturn fault at different slots of dfig. IEEE Access. 2019 Jul 3;7: 89342-53. IEEE Access. 2019 :89342–89353.

[25] Canseven HT, Ünsal A. Performance Improvement of a Five-Phase PMSM Drive Under Open Circuit Stator Faults. 5th IEEE International Symposium on Multidisciplinary Studies and Innovative Technologies (ISMSIT) 2021 Oct 21 (pp. 561-565).

[26] Marzetti MA, Bossio GR, De Angelo CH. Interturn short-circuit fault diagnosis in PMSM with partitioned stator windings. IET Electric Power Applications. 2020 Nov 26; 14(12):2301-11.

[27] Y.S.V. Raman, Dr S. Sri Gowri, Dr B. Prabhakara Rao (2015), Performance Enhancement of Spectral efficiency and throughput with Distributed Dynamic channel allocation using genetic algorithm. IJEER 3(3), 54-57. DOI: 10.37391/IJEER.030303. https://ijeer.forexjournal.co.in/archive/volume-3/ijeer-030303.php

[28] Miska Prasad, A.K Akella (2016), Comparison of Voltage Swell Characteristics in Power Distribution System. IJEER 4(3), 67-73. DOI: 10.37391/IJEER.040302. http://ijeer.forexjournal.co.in/archive/volume-4/ijeer-040302.php